A positron annihilation spectroscopy investigation of magnetically induced changes in defect structures

1990 J. Phys.: Condens. Matter 2 3629

(http://iopscience.iop.org/0953-8984/2/15/018)

J. Phys.: Condens. Matter **2** (1990) 3629–3642. Printed in the UK

A positron annihilation spectroscopy investigation of magnetically induced changes in defect structures

Y Y Su, R F Hochman and J P Schaffer
School of Materials Engineering, Georgia Institute of Technology, Atlanta, GA 30332-0245, USA

Received 2 June 1989, in final form 5 October 1989

Abstract. Positron annihilation spectroscopy (PAS) has been used in conjunction with x-ray analysis to investigate magnetically induced defect recovery in nickel and OFHC copper. Both types of measurement indicate defect recovery during the first few cycles of an applied pulsed magnetic field. In addition, the PAS R-parameter calculations show a change in the dominant defect type during magnetically induced recovery.

1. Introduction

Limited studies over the past few decades have shown the possibility of modifying the properties of metals by using a magnetic field. These investigations have demonstrated that fatigue properties, stress relief, wear resistance and surface composition can be altered by the application of a pulsed magnetic field [1–4].

It has also been determined that a magnetic field treatment can effect the mechanical properties of a variety of materials even at room temperature. For example, Romashev *et al* [5] successfully obtained and observed the martensite γ–α transformation in low-carbon chromium–nickel steel by using a magnetic field without the benefit of a thermal treatment [5]. Cullity *et al* [6] demonstrated the stress relaxation in a nickel specimen loaded in compression. The stress was observed to decreased dramatically with the application of the magnetic field.

Pavlov *et al* [7] used transmission electron microscopy (TEM) to observe differences in the dislocation structure before and after the application of a magnetic field in the paramagnetic metals niobium and molybdenum [7].

The study of magnetically induced recovery of magnetic susceptibility in diamagnetic metals, such as copper, was documented as early as 1946 [8, 9], but only recently has mechanical recovery been reported in an article by Hochman *et al* [10].

Thus, previous studies have demonstrated qualitatively that dislocation movement and annihilation can occur as a result of the application of an external magnetic field. However, neither a quantitative analysis of changes in vacancy concentrations and dislocation structures due to an applied magnetic field nor the mechanisms accountable for these changes have yet been reported.

In this work we have employed positron annihilation spectroscopy (PAS) to study the changes in vacancy and dislocation concentrations and spatial distributions which occur

0953-8984/90/153629 + 14 $03.50

as a result of the application of a pulsed magnetic field. X-ray diffraction was also used for strain analysis of magnetically pulsed material.

2. Background

2.1. Magnetically induced motion of defects

The first theoretical study of the interaction of dislocations with magnetic fields was published by Vicena [11] in 1954. Since that time several additional papers have been published on this topic [12–15]. The application of a magnetic field to a metal causes the angular frequency and spin direction of certain electrons in the metal to change. In ferromagnetic metals, magnetic domains are formed to minimise the sum of several energy terms. These energy terms include exchange forces, magnetocrystalline anisotropy, magnetostatic effects and magnetostriction.

Magnetocrystalline anisotropy is the variation in magnetic properties with crystallographic direction. Owing to this anisotropy the extent of magnetically induced defect recovery may depend on both the direction of the applied magnetic field and the texture of the material under investigation.

The magnetostriction energy term, defined as the elastic strain energy arising from dimensional changes due to magnetisation, results in the development of a complex stress pattern at domain boundaries. As a result, these boundaries can interact with any non-homogeneous stresses in the material.

Regardless of the type of material (ferromagnetic, diamagnetic or paramagnetic), the interaction between a dislocation and the external pulsed magnetic field can change the dislocation free energy. As a result, those dislocations with enhanced free energies may become more mobile. The change in the yield stress associated with an applied magnetic field can be expressed as follows [8]:

$$\sigma = \sigma_0 \exp[-(U_n - \gamma_\alpha - \beta IH)/kT] \tag{1}$$

where U_n is the energy of the potential barrier (activation energy), γ_α is the elastic energy of a dislocation in the external stress field, β is the structure factor, I is the magnetic moment of the dislocation and H is the external magnetic field strength (thus, βIH is the magnetic energy of a dislocation in the magnetic field).

In addition, very low concentrations of impurities such as Fe, Cr and Mn in commercially pure Cu can provide localised magnetic moments [16–22]. These magnetic moments may afford some of the energy necessary to assist in rearrangement and annihilation of dislocation structures in diamagnetic materials.

2.2. Positron annihilation spectroscopy

PAS is a non-contact and non-destructive technique which can be used to characterise the atomic defect structure of materials. Using currently available instrumentation it is possible to investigate:

(i) defect types, distributions and densities,
(ii) the atomic structure of defect such as interstitial–vacancy complexes,
(iii) the size of vacancy clusters,
(iv) the electron density in the vicinity of a vacancy and
(v) extended defects such as dislocations and grain boundaries.

Several review articles have been written on the physics of PAS [23–26]; hence, only a brief review will be presented here. Positrons and electrons are complementary states of matter such that when they encounter one another they will annihilate to produce (usually) two γ-rays. If both particles were at rest, a situation which never arises in real materials, conservation of momentum and energy, would require the two γ-rays to be emitted in exactly opposite directions, each with an energy of 511 keV corresponding to the rest mass of an electron (or positron).

In a typical experiment, positrons are injected from a radioactive source and quickly reach thermal velocities. When the annihilation event occurs, the non-zero net momentum of the positron–electron pair modifies the characteristics of the annihilation radiation. The two γ-rays will have their energies altered from 511 keV and will no longer be emitted in exactly opposite directions.

The technique used in present work is Doppler broadening PAS which measures the deviations from 511 keV. Such measurements can be used to characterise (and under certain conditions to identify) the location of positron 'traps' within the crystal lattice. Since positrons can be preferentially attracted to, and become localised within, open volume and/or negatively charged defect sites, changes in the relative concentrations of such sites will influence the observed annihilation energy lineshapes.

These Doppler PAS energy distributions are usually interpreted using a characteristic lineshape parameter S defined as the sum of the counts in a central region of the peak divided by the total number of counts in the annihilation energy spectrum [27]. In general, for open volume defects such as vacancies and grain boundaries, the electron momentum distribution in the defect region will be narrower than in the (non-defective) bulk (i.e. $S(\text{defect}) > S(\text{bulk})$). Thus, an increase in S (usually) corresponds to an increase in the defect concentration in the specimen.

3. Experimental procedures

3.1. PAS experiments

The positron source for the PAS experiments was about 30 mCi of ^{68}Ge deposited onto a thin (about 0.005 mm) sheet of titanium. Identical specimens were placed on either side of the Ti foil in the standard sandwich configuration. The annihilation energy spectrometer is based on an Ortec coaxial Ge(Li) detector and its associated preamplifier. The remaining components of the system (all from Ortec) include a model 572 main amplifier, model 444 gated bias amplifier, model 918 multichannel buffer and a dedicated IBM personal computer. The energy resolution of this system, as measured by the full width at half-maximum of the 514 keV peak characteristic of ^{85}Sr, is about 1.20 keV. The energy dispersion of the detector was set at 64 eV per channel. The source–detector geometry was fixed and the counting rate was kept constant at approximately 2 kHz (dead time about 3.2%). Each energy spectrum was characterised by the standard 'S'-parameter [27] with a central energy window of 29 channels (1.856 keV) and a total spectrum width of 201 channels (12.864 keV). The stability of the system was determined by checking the data for non-statistical error components [28]. The reported S-parameters represent the average of at least five experiments on each sample pair.

While the S-parameter gives an indication of total defect density, it cannot be used to determine the types of defect present. To overcome this difficulty, Mantl *et al* [29]

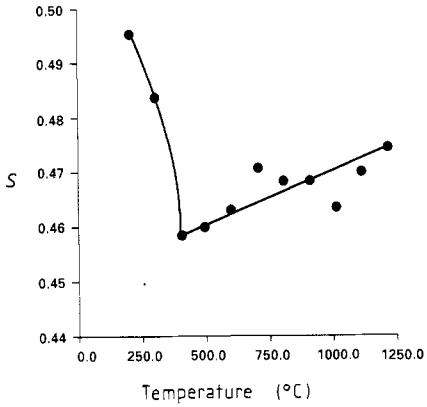

Figure 1. A plot of the PAS *S*-parameter as a function of annealing temperature for a pair of nickel samples initially cold worked to 80% RA. The standard deviation associated with the calculated *S*-parameters is of the order of 4×10^{-4} and is therefore smaller than the data points. The solid line is drawn to guide the eye.

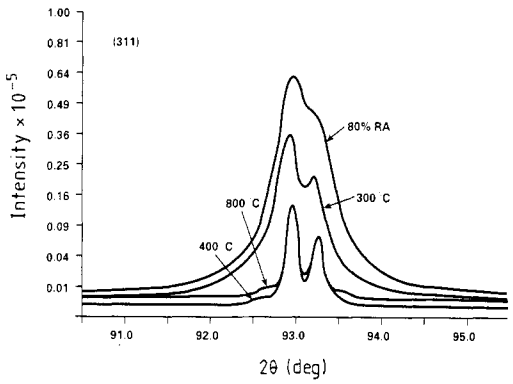

Figure 2. A plot of x-ray intensity versus diffraction condition for one of the nickel samples described in figure 1.

introduced the *R*-parameter which is concentration independent but characteristic of the type of trapping site from which the positron is annihilated. *R* is defined as

$$R = |(I_{V0} - I_V)/(I_{C0} - I_C)| \tag{2}$$

where I_V and I_C are defined as the sums of the counts in the central and wing regions respectively of the peak divided by the total number of counts in the annihilation energy spectrum, and the subscript 0 refers to the reference sample [29].

The following procedure was used to calculate the *R*-parameters. First, for each material investigated, a series of samples were isochronally annealed at various temperatures. These samples were then characterised by both PAS and x-ray diffraction. The sample with the lowest defect density, as measured concurrently by both techniques, was selected as the reference sample (ie. the sample annealed at 400 °C). Typical examples of the PAS and x-ray data are shown in figures 1 and 2. It is interesting to note the *increase* in the *S*-parameter above 400 °C (see figure 1). Although we have not investigated this effect in detail, we can offer the following tentative explanation. As the isochronal annealing temperature increases, the equilibrium vacancy concentration increases. The mobile vacancies can migrate to form vacancy clusters which are retained when the sample is cooled from the annealing temperature. The resulting vacancy clusters are efficient positron traps and will increase the observed *S*-parameter.

Finally, as shown in figure 3, a plot of the difference between the intensities of the normalised annihilation radiation energy distribution curves for a heavily cold-worked sample and the reference sample was used to select the energy windows for calculating I_V and I_C [30]. The width of the central energy window for I_V was 17 channels (1.088 keV) while I_C was defined from channels 30–64 on each side of the peak (total energy width of 4.48 keV).

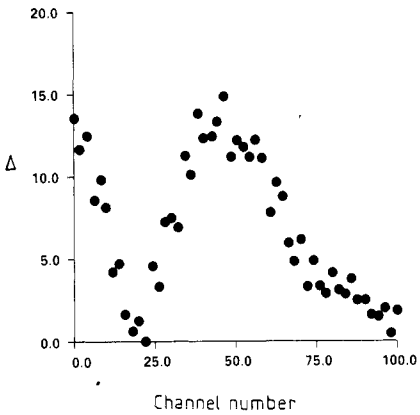

Figure 3. A plot of Δ versus the channel number, where Δ is the magnitude of the difference in the number of counts in the annihilation energy distribution curves for a heavily cold-worked sample and the reference sample.

3.2. *X-ray diffraction experiments*

The x-ray diffraction experiments were performed using a Philips model PW1800 computerised diffractometer. The specific parameters used are an operating voltage of 40 kV, an operating current of 30 mA, a Cu Kα source, a step size of 0.01° and a sampling time of 5 s. The peak position, peak counts, integrated area and strain analysis can all be calculated and plotted within a minute of the conclusion of the experiment.

In order to obtain a completed separation of α_1 and α_2 peaks, a large-angle radiation was chosen for these experiments. This is based on the differentiation and rearrangement of Bragg's law into the form

$$\Delta\theta = (-\Delta d/d)\tan\theta \tag{3}$$

where θ is the nominal Bragg angle, $\Delta\theta$ is the peak shift and Δd is the change in d-spacing compared with the unstrained specimen. Since tan θ increases with an increase in θ, higher values of θ result in an enhanced separation of the α_1 and α_2 peaks.

Mean strain values were calculated using the Warren–Averbach method with the (200)–(400) or (111)–(222) pair reflections.

3.3. *Sample preparation*

Oxygen-free copper (99.99% with 10 ppm oxygen) and commercially pure nickel, obtained from Material Research Corporation, were selected as the materials to be investigated. Each as-received material was treated using the procedure listed below in order to minimise the influence of previous processing and to obtain a uniform grain size.

Step 1. Cold work to 80% reduction in area (RA).
Step 2. Heat treatment at $\frac{2}{3}T_m$ (4 h in argon).
Step 3. Furnace cool.
Step 4. Cold work to desired percentage RA by rolling.

A sample size of 10 mm × 10 mm × 2 mm was cut from the previous cold-worked samples. The specimen surfaces were polished slightly by 1200-grit sandpaper and then subjected to a light acid pickling to prevent the contribution of any surface effects during the PAS experiments [31].

Table 1. Influence of percentage reduction of area (% RA) on the PAS parameters S, R, I_v and I_c for commercially pure nickel.

RA (%)	S	R	I_v	I_c
6	0.4748	0.4998	0.1583	0.1940
11	0.4818	0.4785	0.1611	0.1863
25	0.4871	0.4969	0.1633	0.1839
37	0.4957	0.4887	0.1662	0.1776
50	0.4977	0.5032	0.1674	0.1760
70	0.5032	0.4968	0.1690	0.1724
80	0.5059	0.4727	0.1702	0.1681

After the initial PAS experiments the samples were treated in a pulsed magnetic field of 80 Oe (Fluxatron, model U-102, designed and supplied by Innovex Inc.) for various numbers of cycles. Throughout this paper we shall employ Innovex's definition of a fluxatron cycle. A single fluxatron cycle is actually composed of approximately 315 reversals of magnetic field. The period of each complete reversal is 0.133 s, giving a total cycle time of 42 s.

For the purpose of limiting the temperature rise during magnetic treatment, however, any single pulsed magnetic field (PMF) treatment was limited to a maximum of 10 cycles. The maximum rise in temperature due to PMF treatment was 6 °C. We believe that the corresponding thermal contribution to defect recovery can be neglected in the interpretation of our data. PAS measurements were performed immediately after PMF treatment.

One of the disadvantages of conventional positron sources is that results are limited to the determination of the average defect density in a region which extends from the specimen surface to a depth of 80–150 μm. This is a consequence of the spread in initial kinetic energies of positrons emitted from such sources. In order to gain some information on the spatial distribution of defects before and after PMF treatment, a pair of OFHC copper specimens was subjected to the following procedure.

Step 1. Cold work to 80% RA.
Step 2. Characterise with PAS.
Step 3. Remove approximately 50 μm of material by mechanical polishing.
Step 4. Repeat steps 2 and 3 until a total of 400 μm of material have been removed (the initial thickness of the samples is about 800 μm).

4. Results

Table 1 lists the values of the four PAS lineshape parameters, S, R, I_V and I_C, for the experiments on commercially pure nickel as a function of percentage reduction in area (% RA). Figure 4 is a plot of the S- and R-parameters for these same samples. The errors associated with the S-parameter data ($\pm 1\sigma$) are smaller than the data points. The S data exhibit the well known behaviour of a gradual approach to a saturation value. As expected, the behaviour of I_V is similar to that of S while I_C shows the inverse trend. The

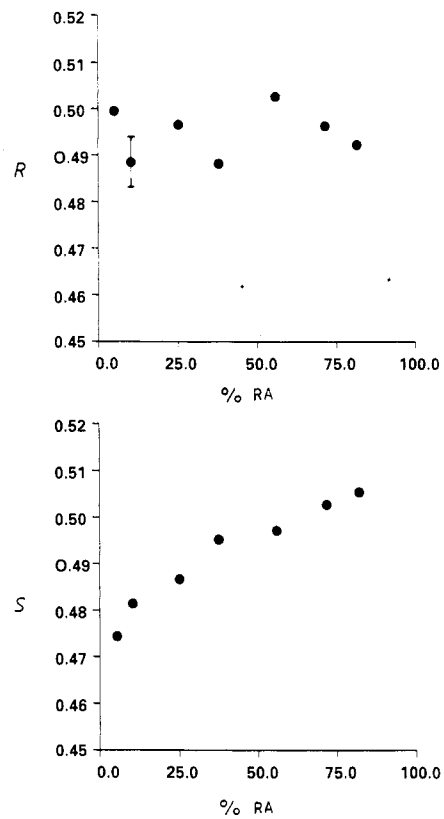

Figure 4. The values of the PAS S- and R-parameters as a function of % RA for a series of cold-worked nickel specimens. The standard deviation associated with the calculated S-parameters is of the order of 4×10^{-4} and is therefore smaller than the data points. A typical error bar ($\pm 1\sigma$) is shown for the R-parameter data.

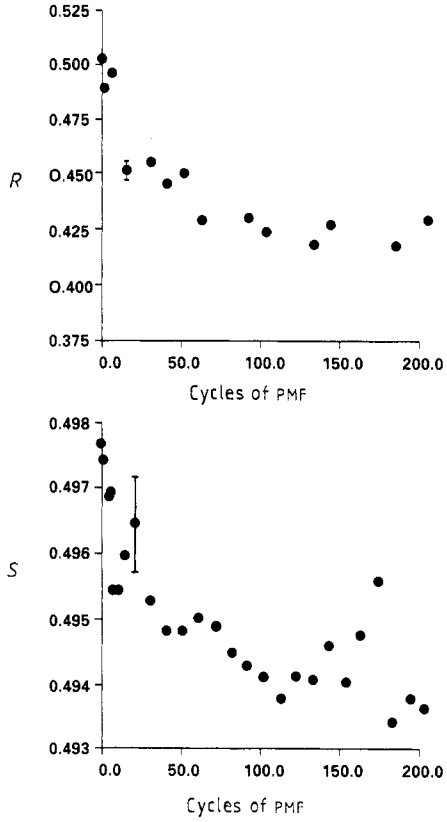

Figure 5. The changes in the PAS S- and R-parameters for the 50% RA nickel samples as a function of number of PMF cycles. Typical $\pm 1\sigma$ error bars are shown.

R-parameter is constant to within experimental error for all levels of % RA (a typical $\pm 1\sigma$ error bar is shown in the figure).

The pair of nickel specimens cold worked to 50% RA were subjected to PMF treatment. The changes in the PAS S- and R-parameters for these samples, as a function of number of PMF cycles, are shown in figure 5. In general, the S-parameter decreases with an increase in the number of PMF cycles. The R-parameter shows a gradual change from about 0.5 to about 0.425.

In order to investigate the dependence of magnetically induced recovery on the amount of prior deformation, the experiments described above were repeated for a sample with 80% RA. The S-parameters for these samples are shown as case 1 in figure 6. Since the initial experiments showed only a minimal change in S with PMF (contrary to the results for the 50% RA samples), a second set of 80% RA samples was investigated. The results of the second set of experiments are shown as case 2 in figure 6. Subsequent x-ray analysis of the two pairs of samples in figure 6 revealed a difference in the texture

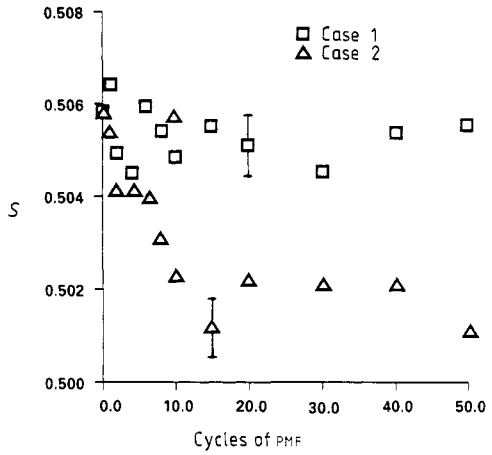

Figure 6. The changes in the PAS *S*-parameters for two sets of 80% RA nickel samples as a function of number of PMF cycles. The primary difference between the two pairs of samples was found to be their texture (see figure 7). Typical $\pm 1\sigma$ errors bars are shown.

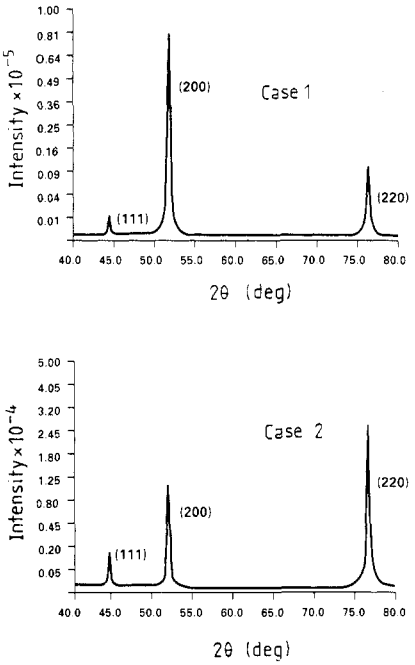

Figure 7. A comparison of plots of x-ray intensity versus diffraction angle for the two sets of nickel specimens described in figure 6. These data suggest a difference in texture between samples.

of the two samples (figure 7). Additional x-ray experiments showed that the texture developed was a strong function of % RA.

A similar set of experiments was performed for OFHC copper. The general trends in the changes in PAS parameters with % RA were similar to those for Ni. That is, the *S*-parameter increased from a value of 0.460 in the annealed condition to a saturation value of about 0.507 after 80% RA. As expected, the behaviour of I_V was similar to that of *S* while I_C decreases to an asymptotic value.

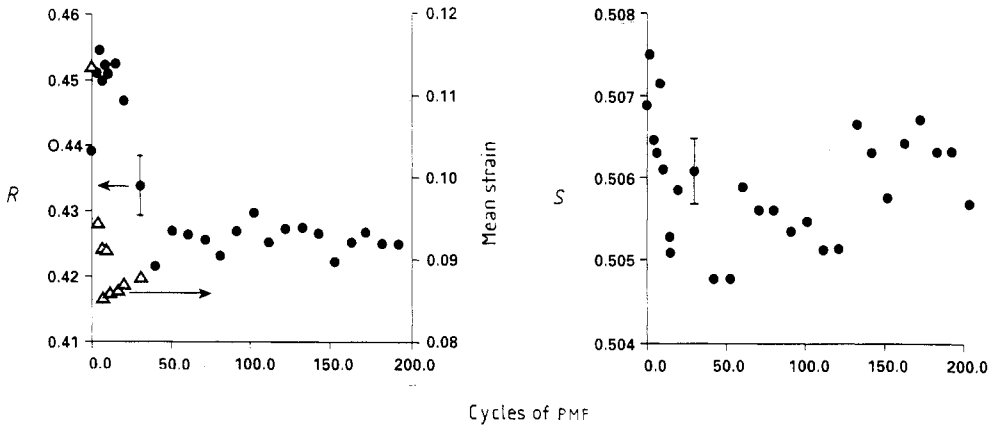

Figure 8. The changes in the mean strain as measured by x-rays and the *S*- and *R*-parameters for the 80% RA OFHC copper samples as a function of number of PMF cycles. Typical $\pm 1\sigma$ error bars are shown.

The changes in the *S*- and *R*-parameters for the 80% RA samples, as a function of number of PMF cycles, are shown in figure 8. The *S*-parameter initially decrease, reaches a minimum value after approximately 50 cycles and then increases again. The *R*-parameter changes abruptly at approximately 40 cycles from a value of about 0.45 to a value of about 0.42–0.43. This step-like change in *R* indicates a change in the dominant defect structure occurring between 35 and 45 PMF cycles. Note that the minimum in *S* occurs at the same number of PMF cycles at which the dominant defect type of changes. Also shown in figure 8 is the change in mean strain, as measured by x-ray diffraction, as a function of the number of PMF cycles. The mean strain decrease from 0 to 10 cycles and then remains essentially constant.

In order to understand the influence of PMF on point defects a pair of OFHC copper samples were heated to 900 °C and quenched in water. The *R*-parameter for these samples, as a function of number of PMF cycles, is shown in figure 9. Note the sharp drop in *R* after only a single PMF cycle.

Figure 10 shows a comparison of the changes in both *S* and *R* for OFHC copper samples (initially cold worked to 80% RA) with and without PMF (100 cycles), as a function of the thickness of the surface layer removed. The *S*-parameters of both pairs of specimens increase as the amount of material removed increases. There is a significant difference in the behaviour of the *R*-parameter for the two material conditions. Figure 11 is a plot of the change in mean strain, as determined from x-ray diffraction, for one of the samples (without PMF) described in the previous figure.

In order to understand the magnetically induced recovery of OFHC copper better, it was decided to compare the results of the previous experiments with the change in the parameter resulting from a thermal anneal. Two pairs of specimens were cold worked to 80% RA. One pair was subjected to 8 PMF cycles and the other pair was annealed at 150 °C for 1 h. Figure 12 is a plot of the *S*-parameter for both pairs of specimens as a function of the thickness of the surface layer removed. In both cases the *S*-parameter is seen to increase as the layer removal thickness increases.

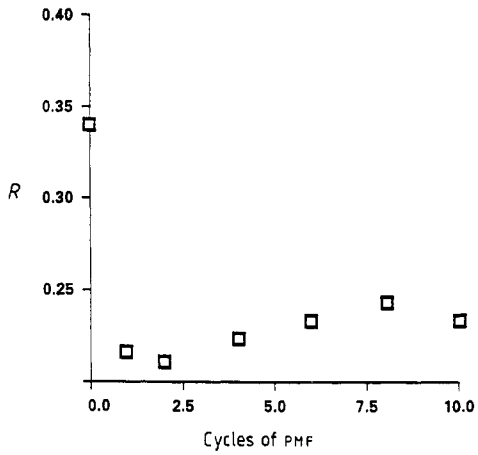

Figure 9. The R-parameter, as a function of number of PMF cycles, for an OFHC copper sample originally water quenched from 900 °C. At this scale the $\pm 1\sigma$ error bars are approximately the same size as the individual data points.

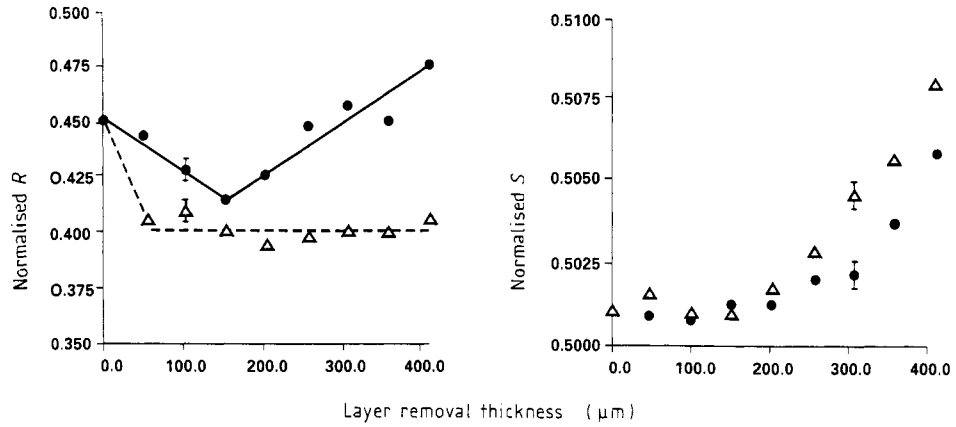

Figure 10. A comparison of the changes in both S and R for samples with (△) and without (●) PMF (100 cycles), as a function of the thickness of the surface layer removed, for OFHC copper samples originally cold worked to 80% RA. Typical $\pm 1\sigma$ error bars are shown. The lines in the figure are drawn only to guide the eye.

5. Discussion

5.1. Commerically pure nickel

The utility of PAS in the characterisation of magnetically induced changes in metallurgical defect structures is related to the sensitivity of the technique to *both* point defects and dislocation structures. As the defect density is increased, there is a corresponding increase in the relative fraction of positrons annihilating from the trapping centres (defects). This results in a continuous increase in the observed S-parameter until a critical defect density is reached. Since essentially all of the positrons are annihilating from the trapped state at the critical concentration, a further increase in defect density will no longer alter the PAS signal. Figure 4 shows the increase in the S-parameter and

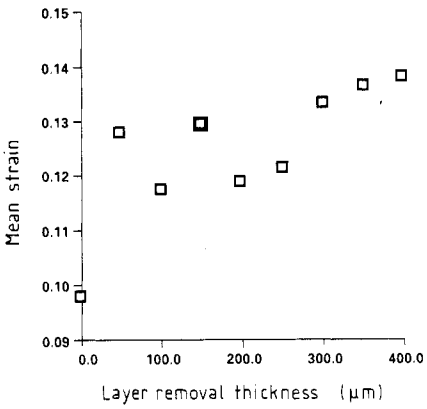

Figure 11. A plot of the change in mean strain, as determined from x-ray diffraction, for one of the samples (without PMF) described in figure 10.

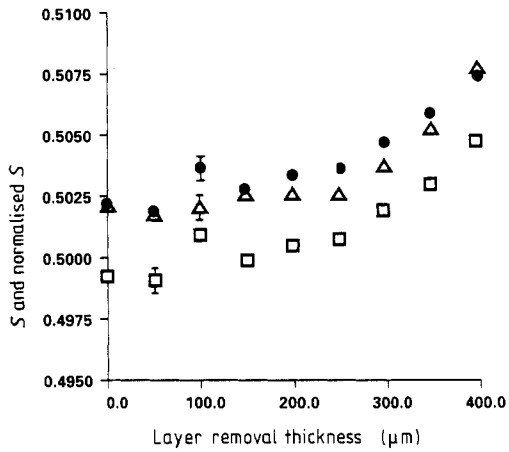

Figure 12. A comparison of S-parameters as a function of the thickness of the surface layer removed for two pairs of specimens of OFHC copper cold worked to 80% RA. One pair was subjected to 8 PMF cycles (△) and the other pair was annealed at 150 °C for 1 h (□). Typical $\pm 1\sigma$ error bars are shown. The normalised data (●) were obtained by adding a constant to each of the raw data points for the heat-treated sample.

an approach to a saturation value as the defect concentration resulting from cold working increases.

In contrast to the S-parameter, the R-parameter responds to changes in the dominant defect type. Figure 4 shows that the R-parameter remains constant to within experimental error over the range of cold working investigated. Since cold work results in a complex defect structure containing both dislocation structures and point defect 'debris' resulting from dislocation interactions, the observed R-value should be intermediate between the characteristic values of dislocations and vacancies. The utility of the R-parameter is that a change in its value indicates a change in the relative concentration of the various defect types.

The data shown in figure 5 indicate magnetically induced defect recovery in Ni samples initially deformed to 50% RA. The decrease in the S-parameter reflects a decrease in the density of positron traps as the number of PMF cycles increases. Most of the recovery occurs during the first 40 cycles. It is interesting to note the existence of a local minimum in the S-parameter data at about 10 cycles of PMF and a local maximum at about 20 cycles of PMF. Although there are several other local maxima and minima in the data, only those at about 10 and about 20 cycles of PMF are reproducible.

In addition to a gradual decrease in the *S*-parameter, the *R*-parameter changes significantly after approximately 15 cycles of PMF. This result reflects a change in the dominant positron trapping state and suggests a change in the relative concentration of defect states. In order to identify the types of defect present, one must obtain reference *R*-values from carefully prepared samples with a known dominant defect type. Such experiments are under way.

The data in figures 6 and 7 suggest an influence of texture on the positron annihilation lineshape parameters. While it is possible that a change in texture will alter the implantation profile of the positron in the nickel, the magnitude of this effect is far too small to explain the data in figure 6. A more likely explanation for the difference in recovery behaviour is the existence of coupling between the direction of the applied magnetic field and the preferred orientation in the polycrystalline sample (i.e. the magnetocrystalline anisotropy). Additional experiments on texture effects are under way.

5.2. Copper

The general trends in the changes in PAS parameters with increasing cold work are similar to those for Ni. That is, S and I_v increase while I_c decreases with increasing % RA until all three parameters approach saturation values at approximately 20% RA.

As indicated by *S*-parameter data, the OHFC material exhibits magnetically induced recovery for all levels of prior cold work (20, 55 and 80% RA). The magnitude of the change in S is, however, smaller than that in nickel.

The data in figure 8 show that in the case of the 80% RA sample, there is a reasonable correlation between the S data and x-ray diffraction data during the first 10–20 PMF cycles. The corresponding *R*-parameter data show a clear change in the relative concentration of the various defect types.

The data in figure 9 show the results of an experiment designed to establish the effect of PMF on quenched-in vacancies in OHFC copper. Note that the *R*-parameter changes significantly after only a single cycle of PMF, indicating a strong interaction between the magnetic field and the as-quenched defect structure. Additional PAS, x-ray and TEM measurements are under way to identify conclusively the defects involved in the recovery process.

Figure 10 shows a comparison of the changes in both S and R for OFHC copper samples (initially cold worked to 80% RA) with and without PMF (100 cycles), as a function of the thickness of the surface layer removed. The *S*-parameter data give in indication of the distribution of defects below the specimen surface. The *S*-values of both pairs of specimens increase as the amount of material removed increases; therefore, the material near the surface was less defective than the underlying material. The major difference between the samples with and without exposure to 100 PMF cycles is the depth at which the defect concentration begins to increase significantly.

The specimens subjected to PMF treatment show a surface layer with a slightly higher *R*-parameter on top of a bulk region with an essentially constant defect structure. In comparison, the *R*-parameter for the material without PMF displays a more complicated behaviour as a function of depth below the surface. Additional experiments of this kind, in conjunction with TEM, should be useful in determining the thickness of the layer of material influenced by the PMF treatment.

6. Conclusions

This study has demonstrated both the viability of magnetically induced defect recovery and the utility of PAS for investigating this phenomenon. The PAS *S*- and *R*-lineshape parameters have been used to investigate changes in defect structures as a function of amount of prior cold work and number of pulsed magnetic field cycles. These results have been correlated with x-ray measurements of mean strain and texture.

Additional experiments are under way in the following areas:

(i) the distribution of defects as a function of distance below the specimen surface,

(ii) a detailed comparison between magnetically and thermally induced defect recovery processes,

(iii) development of a table of defects and corresponding *R*-values to be used (in conjunction with other tools) in defect identification and

(iv) an investigation (both theoretical and experimental) of the effect of texture on magnetically induced defect recovery.

Acknowledgments

The authors wish to acknowledge the Army Research Office for the support of this program through contract DAAL03-88-K-0178. The authors are grateful to Dr Naum Tselesin of Duratech Incorporated (Atlanta, GA) for his helpful comments and to Innovex Incorporated (Hopkins, MN) for supplying the Fluxatron.

References

[1] Finkel V M 1970 *Physics of Failure* (Moscow: Metallurgia)
[2] Finkel V M 1977 *Physical Foundation of Failure Retardation* (Moscow: Metallurgia)
[3] Bose M S C 1984 *Phys. Status Solidi* a **86** 649–54
[4] Evans J F 1986 private communication
[5] Romashev L N, Leont'ev A A, Schastivtsev V M and Sadovskii V D 1984 *Phys. Met. Metallogr. (USSR)* **57** 130–6
[6] Cullity B D and Allen C W 1965 *Acta Metall.* **13** 933–5
[7] Pavlov V A, Pereturina I A and Pecherkina N L 1980 *Phys. Status Solidi* a **57** 449–56
[8] Reekie J and Hutchison T S 1946 *Nature* **157** 807–8
[9] Hutchison T S and Reekie J 1947 *Nature* **158** 537–8
[10] Hochman R F, Tselesin N and Drits V 1988 *Adv. Mater. Processes* **134** 36–41
[11] Vicena F 1954 *Czech. J. Phys.* **5** 480
[12] Chikazumi S 1964 *Physics of Magnetism* (New York: Wiley)
[13] Berkowitz A E and Kneller E 1969 *Magnetism and Metallurgy* vol 2 (New York: Academic)
[14] Scherpereel D E, Kazmerski L L and Allen C W 1970 *Metall. Trans.* **1** 517–24
[15] Cullity B D 1972 *Introduction of Magnetic Materials* (Reading, MA: Addison-Wesley)
[16] Anderson P W 1961 *Phys. Rev.* **124** 41
[17] Wolff P A 1961 *Phys. Rev.* **124** 1030
[18] Jaccarino V and Walker L R 1965 *Phys. Rev. Lett.* **15** 258
[19] Beeby J L 1966 *Phys. Rev.* **141** 781
[20] Graham D G and March N H 1970 *Cryst. Latt. Defects* **1** 121
[21] Dworin L and Narath A 1970 *Phys. Rev. Lett.* **25** 287
[22] Zeller R, Braspenning P J, Deutz J, Podloacky R and Dedericks P H 1982 *Point Defects and Defect Interaction in Metals* ed J Takamura, M Doyama and M Kiritani (Amsterdam: North-Holland)
[23] West R N 1974 *Positron Studies of Condensed Matter* (London: Taylor and Francis)

[24] Dekhtyar I 1974 *Phys. Rep.* **9** 243
[25] Eldrup M 1985 Applications of positron annihilation technique in studies of defects in solids *Defects in Solids* (New York: Plenum)
[26] Lynn K G and Schultz P J 1988 *Rev. Mod. Phys.* **60** 701
[27] Mackenzie I K, Eady J A and Gingerich R R 1970 *Phys. Lett.* **33A** 279
[28] Hara T and Schaffer J P 1988 *J. Phys. E: Sci. Instrum.* **21** 595
[29] Mantl S and Triptshauser W 1978 *Phys. Rev.* B **17** 1645–52
[30] Campbell J L 1977 *J. Appl. Phys.* **13** 365–9
[31] Dave N K and Le Blank R J 1978 *Appl. Phys.* **15** 197–200